Published in final edited form as:
J Immunol. 2011 November 1; 187(9): 4676–4685. doi:10.4049/jimmunol.1101876.

HIV-1 *N*-Glycan Composition Governs a Balance between Dendritic Cell-Mediated Viral Transmission and Antigen Presentation

Thijs van Montfort[*], **Dirk Eggink**[*], **Maikel Boot**[*], **Michael Tuen**[†], **Catarina E. Hioe**[†], **Ben Berkhout**[*], and **Rogier W. Sanders**[*,‡]

[*]Laboratory of Experimental Virology, Department of Medical Microbiology, Center for Infection and Immunity Amsterdam, Academic Medical Center of the University of Amsterdam, 1105 AZ Amsterdam, The Netherlands [†]Department of Pathology, New York University School of Medicine, New York, NY 10010 [‡]Department of Microbiology and Immunology, Weill Medical College, Cornell University, New York, NY 10065

Abstract

The natural function of dendritic cells (DCs) is to capture and degrade pathogens for Ag presentation. However, HIV-1 can evade viral degradation by DCs and hijack DCs for migration to susceptible $CD4^+$ T lymphocytes. It is unknown what factors decide whether a virus is degraded or transmitted to T cells. The interaction of DCs with HIV-1 involves C-type lectin receptors, such as DC-specific ICAM-3–grabbing nonintegrin, which bind to the envelope glycoprotein complex (Env), which is decorated heavily with *N*-linked glycans. We hypothesized that the saccharide composition of the Env *N*-glycans is involved in avoiding viral degradation and Ag presentation, as well as preserving infectious virus for the transmission to target cells. Therefore, we studied the fate of normally glycosylated virus versus oligomannose-enriched virus in DCs. Changing the heterogeneous *N*-linked glycan composition of Env to uniform oligomannose *N*-glycans increased the affinity of HIV-1 for DC-specific ICAM-3–grabbing non-integrin and enhanced the capture of HIV-1 by immature DCs; however, it decreased the subsequent transmission to target cells. Oligomannose-enriched HIV-1 was directed more efficiently into the endocytic pathway, resulting in enhanced viral degradation and reduced virus transfer to target cells. Furthermore, Env containing exclusively oligomannose *N*-glycans was presented to Env-specific $CD4^+$ T cells more efficiently. Taken together, our results showed that the HIV-1 *N*-glycan composition plays a crucial role in the balance between DC-mediated Ag degradation and presentation and DC-mediated virus transmission to target cells. This finding may have implications for the early events in HIV-1 transmission and the induction of antiviral immune responses.

Human immunodeficiency virus-1 infection of target cells is dependent on attachment of the envelope glycoprotein complex (Env) to the cellular receptor CD4 and a chemokine coreceptor, usually CCR5 or CXCR4. $CD4^+$ T lymphocytes are the main target cell for HIV-1 infection, but many other cell types, such as macrophages and dendritic cells (DCs), can also become infected (1).

Address correspondence and reprint requests to Dr. Rogier W. Sanders, Laboratory of Experimental Virology, Department of Medical Microbiology, Center for Infection and Immunity Amsterdam, Academic Medical Center of the University of Amsterdam, 1105 AZ Amsterdam, The Netherlands. r.w.sanders@amc.uva.nl.

Disclosures

The authors have no financial conflicts of interest.

Immature DCs (iDCs) scavenge the mucosal environment for pathogens and are among the first cells to encounter HIV-1 passing the mucosal barrier during transmission (2). iDCs, as professional APCs, capture and internalize pathogens that are subsequently directed to the endocytic pathway to be processed into antigenic peptides. Simultaneous triggering of pathogen-recognition receptors, such as lectin receptors and TLRs, induce DCs to mature and migrate from the mucosa to secondary lymphoid organs. Pathogen-derived peptides are displayed on the cell surface on MHC molecules and are presented to resident T cells to initiate a pathogen-specific immune response (3).

Paradoxically, HIV-1 subverts the natural role of DCs in initiating Ag-specific immune response, by hijacking DCs for passage from the mucosa to the secondary lymphoid organs (4). This facilitates HIV-1 spread to susceptible T lymphocytes, while avoiding degradation and Ag presentation. A fraction of DC-associated HIV-1 evades the degradation pathway by trafficking to a tetraspanin (CD81)-enriched protective environment from where infectious particles can be released to T lymphocytes upon DC–T cell contact (5, 6). Thus, a virus that is taken up by DCs can enter two pathways. First, it can traffic into the endocytic pathway, resulting in viral degradation and Ag presentation. Second, it can avoid degradation by being diverted into a transmission pathway. It is unknown how these pathways are related and what factors determine which pathway the virus enters.

Transmission of DC-captured viral particles to T cells and subsequent infection, termed infection “in trans,” occurs via formation of an “infectious” synapse, where virus is concentrated on the DC side of the synapse, and HIV-1 entry receptors are concentrated on the T cell side (7). In addition to DC-mediated HIV-1 transfer in trans, virus particles can infect DCs directly (infection “in cis”) and spread to T cells via shedding of de novo-produced virions (8). In cis infection of DCs and subsequent spreading to T cells are efficient for CCR5-tropic viruses and is believed to be important for the onset of HIV-1 infection after sexual transmission (9, 10). Later in the course of infection, when Abs impair direct infection of DCs and T cells (11, 12), in trans infection via DCs becomes dominant. This mode of transmission is more efficient for CXCR4-tropic viruses, which may be one explanation for the evolution of CCR5-tropic HIV-1 into the more pathogenic CXCR4 virus type (13).

HIV-1 capture by DCs is mediated by C-type lectin receptors (CLRs) that bind glycosylated structures present on pathogens. CLRs with different specificities, such as the mannose receptor (14), dendritic cell-specific ICAM-3–grabbing nonintegrin (DC-SIGN) (15), blood DC Ag-2, DC-associated C-type lectin 1 and 2 (16, 17), DC immunoreceptor (DCIR) (18), DC-associated lectin-1 (19), C-type lectin receptor (20), DEC-205 (CD205) (21), and macrophage galactose-type lectin (22), can be found on different subclasses of DCs (23). The glycan-binding properties and specificities of these CLRs have been reviewed in detail elsewhere (24). On monocyte-derived iDCs, ~30–50% of the HIV-1 particles are captured by DC-SIGN and DCIR (25–27). DC-SIGN binding is dependent on carbohydrates containing terminal mannose and fucose residues, and particularly high-affinity binding occurs with oligomannose and Lewis structures (28–30).

Almost half of Env’s molecular mass consists of *N*-linked glycans that protect the protein against proteolytic degradation and shield antigenic epitopes from Abs (31–34). *N*-linked glycans on Env are also required for proper folding of the protein and incorporation into viral particles; inhibiting glycosylation impairs protein export from the endoplasmic reticulum (ER) (35). The composition of *N*-linked glycans on Env is highly heterogeneous (Fig. 1). *N*-linked glycans are attached to Env cotranslationally as oligomannose structures that are trimmed and modified during transit through the ER and Golgi, giving rise to a variety of carbohydrates. A number of *N*-glycans on Env are resistant to mannose trimming

in the ER and Golgi and retain an oligomannose composition (36, 37). Thus, Env is decorated with a mixture of oligomannose and complex *N*-glycans, which may have an important impact on the interaction with DCs and subsequent transmission to $CD4^+$ T lymphocytes.

We hypothesized that the particular composition of HIV-1 *N*-glycans plays a role in deciding the fate of the virus that is captured by DCs. Therefore, we investigated the consequences of changing the HIV-1 Env *N*-glycan composition to exclusively oligomannose. Oligomannose-enriched HIV-1 bound DC-SIGN more efficiently and viral capture by DCs was strongly increased. DC-captured virus enriched with oligomannose glycans was also more efficiently targeted to the endosomal pathway, where viral particles were degraded. As a result, the transfer of infectious virus particles to susceptible target cells was strongly impaired. Moreover, Env with only oligomannose *N*-linked glycans was more efficiently presented to cognate T cells. Collectively, these results demonstrated that the HIV-1 Env *N*-glycan composition plays a role in HIV-1 binding to iDCs and determines whether the virus is degraded for Ag presentation or is transmitted to $CD4^+$ target T cells.

Materials and Methods

Plasmids

Expression plasmids for monomeric LAI and JR-FL gp120 and trimeric JR-FL gp140 are described elsewhere, as are the plasmids encoding the entire HIV-1 genome of CCR5-tropic JR-CSF and CXCR4-tropic LAI (38, 39). The enhanced GFP (EGFP)-vpr plasmid was a kind gift from Thomas Hope (University of Illinois Medical Center, Chicago, IL).

Reagents

DC-SIGN–Fc was purchased from R&D Systems (Minneapolis, MN). HIV-Ig was obtained through the AIDS Research and Reference Reagent Program, Division of AIDS, National Institute of Allergy and Infectious Diseases, National Institutes of Health (Bethesda, MD). mAb 2G12 was obtained from Hermann Katinger, through the AIDS Research and Reference Reagent Program. CD4-IgG2 and anti-V3 gp120 mAb PA1 were gifts from Bill Olson (Progenics Pharmaceutical, Tarrytown, NY). mAbs against CD81, DC-SIGN, EEA1, CD63, and LAMP-1 to stain-specific DC compartments were obtained from BD Pharmingen (San Jose, CA). AffiniPure donkey anti–mouse-Cy5 was acquired from Jackson ImmunoResearch (Suffolk, U.K.) and used at a 200-fold dilution. Nuclear DNA was stained with Hoechst 33258 (Sigma Aldrich, Zwijndrecht, The Netherlands).

Cells

293T, 293S $GnTI^{-/-}$, and TZM-bl cells were cultured and maintained in DMEM (Invitrogen, Breda, The Netherlands); Raji and Raji cells expressing DC-SIGN (Raji–DC-SIGN cells) were cultured and maintained in RPMI 1640 (Invitrogen). Medium contained 10% heat-inactivated FCS (HyClone, Perbio, Etten-Leur, The Netherlands), MEM nonessential amino acids (0.1 mM; Invitrogen), and penicillin/streptomycin (both at 100 U/ml). iDCs were prepared from human blood monocytes isolated from buffy coats by Ficoll-gradient sedimentation, followed by a magnetic bead CD14-selection step using a cell-sorting system (Miltenyi Biotec, Bergisch Gladbach, Germany). Purified monocytes were cultured in RPMI 1640 containing 10% FCS and were differentiated into iDCs by stimulating the cells twice with 45 ng rIL-4/ml (Biosource, Nivelles, Belgium) and GM-CSF (500 U/ml; Schering-Plough, Brussels, Belgium) on days 0 and 4; they were used on day 6.

Env and virus production

293T and 293S GnTI$^{-/-}$ cells were transiently transfected with plasmids expressing recombinant Env or complete HIV-1 using linear poly-ethylenimine (PEI; m.w. 25,000; Polysciences Europe, Eppelheim, Germany) in the presence or absence of 100 μM kifunensine (Calbiochem, Merck, Darmstadt, Germany), as described (40). Briefly, plasmid DNA was diluted in 1/10 of the final culture volume of DMEM and mixed with PEI (0.15 mg/ml final concentration). After incubation for 20 min, the DNA-PEI mix was added for 4 h to the cells before replacement with normal culture medium. Supernatants were harvested 48 h after transfection with Env or 72 h after transfection with virus plasmids and frozen in aliquots. The viral CA-p24 protein in supernatant was quantified by ELISA and used to standardize virus input at subsequent experiments.

EGFP-labeled JR-CSF was produced on 293T cells and transfected with JR-CSF and EGFP-vpr plasmids (1:1 ratio) using Lipofectamine 2000, according to the manufacturer's protocol (Invitrogen, Carlsbad, CA), in the presence or absence of kifunensine. Viral supernatant was harvested 72 h posttransfection and concentrated 10 times using Amicon Ultra filters (100k; Millipore, Carrigtwohill, Ireland).

gp120 and trimer ELISA

Microlon 96-well plates (Greiner Bio-One, Alphen aan den Rijn, The Netherlands) were coated with 100 μl anti-gp120 Ab D7324 (10 μg/ml; Aalto Bioreagents, Dublin, Ireland), in 0.1 M $NaHCO_3$ (pH 8.6) (100 μl/well). Plates were washed twice with TBS, and wells were blocked with 1% BSA in TBS for 1 h. Env supernatant was diluted three times in TBS containing 10% FCS, and 100 μl/well was used for Env binding to D7324 for 2 h at room temperature. Protein binding sites were blocked with 20 mM Tris, 150 mM NaCl, 1.0 mM $CaCl_2$, 2.0 mM $MgCl_2$ (tris saline magnesium buffer [TSM]) containing 5% BSA. Serially diluted HIV-Ig, 2G12, DC-SIGN–Fc, or CD4-IgG2 in TSM/5% BSA was added for 2 h, followed by three washes with TSM, supplemented with 0.05% Tween-20. HRP-labeled goat-anti-human IgG (0.2 μg/ml; Jackson ImmunoResearch) was added for 30 min in TSM/5% BSA, followed by five washes with TSM/0.05% Tween-20. Colorimetric detection was performed using a solution containing 1% 3,3′,5,5′-tetramethylbenzidine (Sigma-Aldrich), 0.01% H_2O_2 in 0.1 M sodium acetate, 0.1 M citric acid. The colorimetric reaction was stopped using 0.8 M H_2SO_4, and light absorption was measured at 450 nm.

SDS-PAGE and Western blotting

SDS-PAGE and Western blotting were performed, as previously described (38). Primary PA1 mouse mAb (0.2 μg/ml) and secondary HRP-labeled goat anti-mouse IgG (1:5000 dilution) were used to detect the Env with Western Lightning ECL solution (PerkinElmer, Groningen, The Netherlands).

Virus infectivity

TZM-bl cells were cultured to 70–80% confluency in a 96-well plate. Cells were washed once with PBS before virus infection (5 ng/ml CA-p24) in the presence of 400 nM saquinavir (Roche, Basel, Switzerland) and DEAE-dextran (Sigma) at 40 μg/ml in a total volume of 200 μl. The medium was removed 2 d postinfection, and cells were washed once with PBS before lysis with Reporter Lysis Buffer (Promega, Madison, WI). Luciferase activity was measured with the Glomax luminometer using the Luciferase Assay kit (Promega), according to the manufacturer's instructions (Turner BioSystems, Sunnyvale, CA). All infections were performed in triplicate. Background luciferase activity was determined using uninfected cells and was subtracted from experimental samples. We also performed infectivity experiments in the absence of DEAE to exclude that its presence

affected the relative infectivity of variationally glycosylated virus. We found that it did not (data not shown).

Virus capture

A total of 1×10^6 Raji or Raji–DC-SIGN cells or 3×10^5 iDCs treated or not with mannan (30 μg/ml) for 30 min were incubated for 2 h with JR-CSF or LAI HIV-1 (15 ng/ml CA-p24). The cells were washed three times with PBS to remove unbound virus and then lysed in 1% Empigen detergent for 1 h at 56°C. Cell debris was removed by centrifugation, and CA-p24 levels were determined by ELISA. EGFP-labeled JR-CSF HIV-1 (100 ng/ml CA-p24) was incubated for 2 h with 2×10^5 iDCs. Cells were washed twice and prepared for confocal analyses, as previously described (26).

Confocal microscopy

Fluorescent images were generated with a Leica DM SP2 AOBS confocal microscope with an ×63 HCX PL APO 1.32 oil objective. We randomly selected three fields, each containing ~20 cells, and analyzed the colocalization in 50–60 cells. Cells were scanned from top to bottom in 20 frames (512 × 512), with a pixel size of 232 nm and a step size of 340 nm. Images with a line average of two scans per image were acquired with the Leica confocal image-processing software. Colocalization was analyzed using a semiautomatic program based on DipImage (Technical University Delft, The Netherlands), custom-written in Matlab (Mathworks, Natick, MA). Briefly, the Isodata algorithm was used to determine the threshold for positive pixels. Colocalization was determined as the percentage of overlapping pixels for each cell.

HIV-1–transmission assay

For transmission experiments, 1×10^5 iDCs treated or not with mannan or Raji or Raji–DC-SIGN cells were incubated for 2 h with virus (3 ng/ml CA-p24). Unbound virus was removed by washing the cells three times with RPMI 1640 medium supplemented with 10% FCS. The cells were cocultured with TZM-bl reporter cells for 48 h in the presence of 400 nM saquinavir and 40 μg/ml DEAE. HIV-1 transfer and infection of reporter cells was quantified by measuring luciferase activity.

Virus degradation

iDCs were inoculated with JR-CSF or LAI HIV-1 (25 ng/ml CA-p24) for 2.5 h at 37°C. Unbound virus was removed by washing cells three times with cold (4°C) medium. DCs were plated in duplicate in a 96-well plate (3×10^5 per well) in 50 μl medium at 4°C. The temperature was quickly raised to 37°C, and viral degradation was stopped by lysing cells through addition of 50 μl 1% Empigen at different time intervals. The amount of remaining CA-p24 was determined by ELISA.

gp120-specific T cell proliferation

gp120-specific $CD4^+$ T cells, reactive to the C2 peptide PKISFEPIPI-HYCAPAGFAI, were described previously (41). Triplicate wells of HLA-matched iDCs (50×10^3) were inoculated with mock supernatant, Env-containing supernatant, or C2 peptide (8 ng/ml; PKISFEPIPIHYCA-PAGFAI)-containing mock supernatant in a 96-well plate for 30 min before the addition of 50×10^3 PS02 T cells. Ten kilobecquerel radioactive tritium thymidine (PerkinElmer, Boston, MA) was added on day 2, and the incorporation of tritium into cellular DNA was allowed for 16 h. Cells were blotted on paper and washed five times to remove free tritium. The cells on paper were submerged in Ultima Gold scintillation fluid (PerkinElmer), and the radioactivity was measured with a liquid scintillation counter. T cell proliferation was also measured by FACS. Quadruplicate samples of iDCs (5×10^4) were

incubated with Env culture supernatant for 2 h at 37°C in a 96-well plate and washed twice with PBS to remove unbound Env. The cells were then mixed with PS02 T cells (5×10^4) and cocultured for 6 d. T cells were stained with CD3-allophycocyanin, and cell proliferation was analyzed by FACS flow cytometry by counting living $CD3^+$ T cells in 50 μl volume.

Statistical analysis

All statistical comparisons were performed using the unpaired *t* test (two-tailed).

Results

Enrichment of oligomannose *N*-glycans on Env enhances DC-SIGN binding

To study the role of *N*-glycan composition of HIV-1 Env on capture and transmission by iDCs, we produced monomeric and trimeric HIV-1 gp120 and gp140 in 293T cells in the presence ($gp120_{kif}$ and $gp140_{kif}$) or absence of kifunensine ($gp120_{wt}$ and $gp140_{wt}$). Kifunensine is a mannose analog that inhibits mannosidase I, which is required for the cleavage of terminal mannose residues from *N*-linked glycans, thereby uniformly preserving $Man_9GlcNAc_2$ glycans (42). HIV-1 gp120 and gp140 were also produced in 293S $GnTI^{-/-}$ cells ($gp120_{GnTI}{}^{-/-}$ and $gp140_{GnTI}{}^{-/-}$), which lack the GlcNAc transferase I enzyme (GnTI) required for addition of a GlcNAc group to $Man_5GlcNAc_2$ *N*-glycans. As a consequence further processing of *N*-glycans is arrested, resulting in the formation of a mixture of $Man_{5–9}GlcNAc_2$ *N*-glycans (43). Thus, $gp120_{kif}$ and $gp120_{GnTI}{}^{-/-}$ are devoid of complex *N*-glycans, but are enriched in oligomannose *N*-glycans with different numbers of mannose residues per glycan (Fig. 1*B*). JR-FL and LAI gp120, as well as JR-FL gp140, could be produced efficiently in transiently transfected cells, but the migration on SDS-PAGE gels differed, consistent with the presence of different glycoforms (Fig. 2*A*, data not shown). The highest m.w. was observed for wild-type gp120 produced on 293T cells containing a heterogeneous mixture of complex and oligomannose carbohydrates. $gp120_{kif}$ had a slightly lower m.w. than $gp120_{wt}$. The smallest m.w. was observed for $gp120_{GnTI}{}^{-/-}$ containing a mixture of $Man_{5–9}GlcNAc_2$ glycans (Fig. 2*A*).

DC-SIGN binds oligomannose glycans efficiently and has been implicated in HIV-1 capture and transmission (44). We performed ELISA assays to study whether the alteration of the *N*-glycan composition on Env affects the affinity for DC-SIGN or Env-specific conformational mAbs. Monomeric gp120 (LAI and JR-FL) and trimeric Env (JR-FL) produced on 293T cells with kifunensine interacted more efficiently with DC-SIGN than did Env_{wt} (Fig. 2*B*), by 2-fold for both gp120s and 5-fold for trimeric JR-FL. The 2G12 mAb, which targets a cluster of oligomannose *N*-glycans on Env (37, 45), also bound more strongly to trimeric Env produced in the presence of kifunensine (Fig. 2*C*). To assess whether modulation of the *N*-glycan composition affected the overall conformation of Env, we measured the binding of pooled sera from HIV^+ individuals (HIV-Ig) and the CD4 mimetic, CD4-IgG2 (Fig. 2*D*). In the absence or presence of kifunensine, binding of HIV-Ig to Env was identical, as was binding of CD4-IgG2. These results demonstrated that Env production in the presence of kifunensine enhanced the binding to DC-SIGN, but it did not affect conformational epitopes of other regions of Env.

To provide further evidence that oligomannose-enriched Env has a higher affinity for DC-SIGN, we coated both $gp120_{wt}$ and $gp120_{kif}$ onto an ELISA plate and measured DC-SIGN binding in the presence of serial dilutions of mannan (Fig. 2*E*). High concentrations of mannan could almost completely block the binding of DC-SIGN to $gp120_{wt}$, but the same concentration of mannan only weakly blocked DC-SIGN binding to $gp120_{kif}$. In an alternative experiment, we coated ELISA plates with $gp120_{wt}$ and $gp120_{kif}$ and measured

DC-SIGN binding in the presence of trimeric $gp140_{wt}$ or $gp140_{kif}$ as the competitors (Fig. 2*F*). We used His-tagged gp140 trimers as competitors because they lack the D7324 tag and cannot bind to the D7324-coated ELISA plates. Trimeric $gp140_{kif}$ inhibited DC-SIGN binding to $gp120_{wt}$, but $gp140_{wt}$ did not (Fig. 2*F*, *left panel*). Furthermore, none of the competitors could block the binding of DC-SIGN to $gp120_{kif}$ at the concentrations used (Fig. 2*F*, *right panel*). These data confirmed that oligomannose-enriched Env has a higher affinity for DC-SIGN compared with Env_{wt}.

N-glycan manipulation does not affect HIV-1 infectivity

We next tested whether modified Env *N*-glycans affected the infectivity of HIV-1. This was assayed on the HIV-1–susceptible TZM-bl reporter cell line that expresses the CD4, CCR5, and CXCR4 receptor and contains a luciferase reporter gene under control of the HIV-1 long terminal repeat promoter. The infectivity of the CCR5-tropic JR-CSF strain, produced in the absence of kifunensine (JR-CSF_{wt}) or the presence of kifunensine (JR-CSF_{kif}), was identical. JR-CSF produced on $GnTI^{-/-}$ cells (JR-$CSF_{GnTI}{}^{-/-}$) also showed no difference in infectivity compared with either JR-CSF_{wt} or JR-CSF_{kif} (Fig. 3*A*). Similarly, no difference in infectivity was observed for CXCR4-tropic LAI_{wt}, $LAI_{GnTI}{}^{-/-}$, and LAI_{kif}. To test whether infectivity was dependent on viral input, we serially diluted virus stocks and measured the infectivity (Fig. 3*B*). Again, the infectivity was identical for wt-, kifunensine–, or $GnTI^{-/-}$–produced virus for both the CCR5- and CXCR4-tropic HIV-1 strain. These data illustrated that modulation of HIV-1 Env glycosylation does not affect Env function and viral infection of TZM-bl cells.

Enrichment of oligomannose *N*-glycans enhances virus capture by Raji–DC-SIGN cells and iDCs

We explored the effect of oligomannose enrichment on virus binding to DC-SIGN expressing cells. The efficiency of HIV-1 binding to DC-SIGN was measured by detection of viral CA-p24 captured by Raji–DC-SIGN cells (Fig. 4*A*). JR-CSF_{kif} was most efficiently captured, followed by JR-$CSF_{GnTI}{}^{-/-}$ and JR-CSF_{wt}. Likewise, the oligomannose-enriched LAI variants LAI_{kif} and $LAI_{GnTI}{}^{-/-}$ were also more efficiently captured compared with LAI_{wt}. Thus, viruses containing more oligomannose *N*-glycans are more efficiently captured by Raji–DC-SIGN cells. DCs are likely to play a role in the onset of HIV-1 infection (10, 46); therefore, we analyzed the effect of Env glycan modification on HIV-1 capture by monocyte-derived iDCs. JR-$CSF_{GnTI}{}^{-/-}$ and JR-CSF_{kif} were more efficiently captured by iDCs than was JR-CSF_{wt} (Fig. 4*B*). Inhibiting mannose-dependent HIV-1 capture with excess of mannan as competitor completely negated the enhanced capture of both JR-$CSF_{GnTI}{}^{-/-}$ and JR-CSF_{kif}, confirming the importance of DC-SIGN or other mannose-recognizing lectins on iDCs in HIV-1 capture (Fig. 4*B*). We noted that, irrespective of the glycan composition, LAI virus was more efficiently captured by DC-SIGN–expressing cells than was JR-FL virus. This is consistent with previous findings that CXCR4-using viruses are generally more efficiently captured and transmitted by monocyte-derived iDCs compared with CCR5-using viruses (13).

The enhanced capture of JR-CSF_{kif} by iDCs was corroborated in confocal-microscopy experiments by studying capture of GFP-labeled virus (Fig. 4*C*). An ~2-fold increase in JR-CSF_{kif} capture was observed in comparison with JR-CSF_{wt} (Fig. 4*D*), consistent with the CA-p24 measurements.

Enrichment of oligomannose glycans reduces viral transmission to target cells

HIV-1 captured by iDCs or Raji–DC-SIGN cells can be transferred in trans to susceptible T lymphocytes. To assess whether HIV-1 Env glycan modification affects viral transfer, we loaded Raji–DC-SIGN cells with the differently glycosylated HIV-1 particles and measured

viral transfer to TZM-bl cells. JR-CSF$_{wt}$ virus was efficiently transferred to the permissive reporter cell line (Fig. 5*A*). On the contrary, the more efficiently captured JR-CSF$_{GnTI}^{-/-}$ and JR-CSF$_{kif}$ viruses were transferred less efficiently, with the lowest transmission efficiency obtained with JR-CSF$_{kif}$ (Fig. 5*A*). Similar results were obtained with the CXCR4-tropic LAI (Fig. 5*B*). No virus transmission was observed with the control Raji cells lacking DC-SIGN. These results demonstrated that enhanced viral binding to DC-SIGN can hamper efficient transfer to target cells.

We examined the viral transfer by iDCs to determine the effect of HIV-1 glycan modification on binding to naturally expressed CLRs. Consistent with previous studies, JR-CSF$_{wt}$ was efficiently transferred by iDCs (13) (Fig. 6*A*). On the contrary, JR-CSF$_{kif}$ was transmitted to TZMbl cells 10-fold less efficiently compared with JR-CSF$_{wt}$ (Fig. 6*A*), consistent with the Raji–DC-SIGN cell whereas JR-CSF$_{GnTI}^{-/-}$ virus displayed an experiments (Fig. 5), intermediate phenotype. Inhibiting HIV-1 capture with mannan as competitor significantly reduced HIV-1 transfer of JR-CSF$_{wt}$ by 3.3-fold. The low transmission efficiency of JR-CSF$_{kif}$ could be further reduced (by 2.2-fold) by treating the iDCs with excess mannan, whereas transmission of JR-CSF$_{GnTI}^{-/-}$ virus was reduced by 4.4-fold upon mannan treatment. The differences in the efficiency of mannan blockade may reflect differences in DC-SIGN affinity and/or avidity (Fig. 2*E*, 2*F*).

Transmission of the LAI$_{kif}$ virus by iDCs was also strongly decreased compared with LAI$_{wt}$ (by ~10-fold), and transmission of LAI$_{GnTI}^{-/-}$ virus was also reduced (Fig. 6*B*). Treating iDCs with mannan further reduced transmission of all LAI variants (Fig. 6*B*), as was seen for the JR-CSF variants (Fig. 6*A*). Collectively, these results illustrated that enhanced HIV-1 capture by DC-SIGN–expressing cells, such as Raji–DC-SIGN cells and iDCs (Fig. 4*A*, 4*B*), does not necessarily result in enhanced transmission to infectable target cells. It seems then that a balanced glycan composition, including both oligomannose and complex glycans, is required for optimal exploitation of CLRs and efficient virus transmission.

Oligomannose-enriched virus colocalizes with endocytic markers in iDCs

Pathogen-recognition receptors, such as DC-SIGN on iDCs, are involved in Ag capture and subsequent degradation for Ag presentation. A proportion of captured HIV-1 particles reside in a CD81 (tetraspanin)-enriched DC environment and escape proteolytic degradation (5, 6, 47). To evaluate the role of Env *N*-glycan composition in the processing of HIV-1 by iDCs, we used confocal microscopy to analyze the colocalization of fluorescent JR-CSF$_{wt}$ and JR-CSF$_{kif}$ with markers for the plasma membrane and endocytic compartments. Colocalization of HIV-1 with specific markers was quantified, and representative photographs of single cells are shown (Fig. 7*A*). The overlay of HIV-1 with a specific compartment was assessed as a percentage of total virus particles for each individual cell (Fig. 7*B*). Approximately, 20–25% of the JR-CSF$_{wt}$ particles colocalized with DC-SIGN or CD81. These two markers are predominantly localized on the plasma membrane, but they can be internalized by endocytosis (5). Similar results were obtained for JR-CSF$_{kif}$ (Fig. 7*B*). These results demonstrated that a large proportion of captured viral particles are trapped on or near the plasma membrane. A relatively small amount of JR-CSF$_{wt}$ was clustered with EEA1 (~3%) and CD63 (~4%), which mark early and late endosomes, respectively. Oligomannose-enriched virus colocalized more consistently with both EEA1 and CD63 (~8 and ~12%, respectively). The relatively low colocalization of both viruses with EEA1 and CD63 may be, in part, a consequence of fast transit through these compartments, but the colocalization of oligomannose-enriched virus with these markers was consistently higher. Colocalization of both JR-CSF$_{wt}$ and JR-CSF$_{kif}$ in the lysosomal LAMP-1 compartment was ~11%. The percentage of HIV-1 associated with the LAMP-1 compartment can be underestimated, because ongoing virus degradation in the lysosome impedes visualization of intact HIV-1 particles. Indeed, we observed stronger colocalization when we costained for LAMP-1 and

CA-p24, which represents intact, as well as degraded, virus (data not shown). Collectively, the increased colocalization of HIV-1_{kif} in the EEA1 and CD63 compartment showed that oligomannose-enriched virus is more efficiently directed into the endocytic pathway compared with JR-CSF_{wt} virus in iDCs.

Oligomannose-enriched virus is more rapidly degraded by iDCs

The increased targeting of oligomannose-enriched virus to the endocytic pathway in iDCs (Fig. 7) might imply that oligomannose-enriched virus is more efficiently degraded, explaining the reduced transmission, despite the enhanced virus capture. Based on viral CA-p24 values, we measured the degradation rate of JR-CSF and LAI in iDCs over a period of 72 h. iDCs loaded with JR-CSF_{wt} degraded 50% of the captured virus ($t_{1/2}$) within 159 min (Fig. 8*A*). Degradation of JR-CSF_{kif} was remarkably faster, with a $t_{1/2}$ of 38 min (Fig. 8*A*). LAI_{kif} ($t_{1/2}$ of 70 min) was also degraded more rapidly than LAI_{wt} ($t_{1/2}$ of 599 min) in iDCs (Fig. 8*B*). The difference between the degradation of CCR5-tropic and CXCR4-tropic viruses is consistent with a report showing that CXCR4-tropic HIV-1, such as LAI, is degraded less efficiently in iDCs than a CCR5-tropic virus, such as JR-CSF (5). Importantly, these results illustrated that virus particles enriched with oligomannose glycans are more efficiently targeted to the endocytic pathway and are degraded more rapidly.

Oligomannose-enriched Env induces stronger DC-mediated Env-specific T cell proliferation

Because oligomannose-enriched virus is more efficiently captured by DCs and more rapidly degraded, we hypothesized that the *N*-glycan composition on the Env could influence Ag processing and presentation to T cells. To measure Ag presentation, we used the Env-specific PS02 T cell line, which recognizes a peptide derived from the C2 region of gp120 (41). PS02 T cells were mixed with HLA-matched iDCs in the presence of mock supernatant, $gp140_{wt}$-containing supernatant, or a specific C2-derived peptide (Fig. 9*A*). In these cocultures, $gp140_{wt}$ and the C2 peptide induced proliferation of PS02 cells, whereas mock supernatant did not (Fig. 9*A*).

To determine whether Env *N*-glycan composition influences Ag presentation by DCs and subsequent T cell proliferation, we fed $gp120_{wt}$ and $gp140_{wt}$ or $gp120_{wt}$ and $gp140_{wt}$ or $gp120_{kif}$ and $gp140_{kif}$ to HLA-matched iDCs to allow for Ag processing, followed by a wash step to remove unbound Env and coculturing with PS02 cells. DCs pulsed with monomeric JR-FL gp120 and trimeric JR-FL gp140 containing exclusively oligomannose *N*-glycans triggered T cell proliferation more efficiently compared with DCs incubated with their normally glycosylated counterparts ($p < 0.01$; Fig. 9*B*), suggesting that an increase in oligomannose content enhances Ag processing and presentation by DCs.

Discussion

We studied the influence of HIV-1 Env *N*-glycan composition on viral transmission from DC-SIGN–expressing cells and iDCs to infectable target cells. Oligomannose-enriched HIV-1 was generated by production in 293T cells in the presence of the glycan-processing inhibitor kifunensine, resulting in the formation of homogeneous $Man_9GlcNAc_2$ *N*-glycans. As an alternative approach, we expressed virus in 293S $GnTI^{-/-}$ cells that lack the GnTI enzyme, resulting in generation of $Man_{5–9}GlcNAc_2$ *N*-glycans on Env (38, 43). The elimination of complex *N*-glycans did not compromise Env production, conformation, and/or entry function, in agreement with previous studies (32, 38, 48, 49). However, we showed in this study that changing the *N*-glycan composition of Env had dramatic effects on the interaction of HIV-1 with iDCs. Specifically, enrichment of oligomannose glycans enhanced HIV-1 capture by iDCs, but it impaired transmission to HIV-1–susceptible cells. The

reduced transmission can be explained by enhanced trafficking through the endocytosis pathway and enhanced virus degradation (Figs. 7, 8). The enhanced degradation of oligomannose-enriched Ag is accompanied by enhanced proliferation of Env-specific T lymphocytes (Fig. 9).

Enhanced capture of oligomannose-enriched HIV-1 by iDCs was mediated by CLRs, such as DC-SIGN, because blocking of these receptors with mannan reduced the increased capture. Mannan blocking did not completely block capture of HIV-1. This is caused, in part, by a higher affinity of DC-SIGN for oligomannose *N*-glycans than for soluble mannan; however, it can also be explained by the fact that receptors with specificities, other than mannose, contribute to HIV-1 capture, such as galactosyl ceramide or the heparan sulfated syndecan-3 receptor on monocyte-derived iDCs (50–52).

We found that Env binding to mannan-sensitive receptors, such as DC-SIGN, was increased when the protein was produced on 293T cells in the presence of kifunensine. Furthermore, we observed that DC-SIGN–expressing cells captured kifunensine virus more efficiently than $GnTI^{-/-}$-derived virus. DC-SIGN interacts with the outer trimannose core on $Man_{5-9}GlcNAc_2$ sugars, and high affinity is observed when additional α1–2-linked mannoses are present (29, 53). These α1–2-linked mannoses are less abundant on *N*-glycans produced on $GnTI^{-/-}$ cells compared with *N*-glycans formed by 293T cells in the presence of kifunensine (38). Therefore, the observed differences in DC-SIGN binding for the two types of oligomannose-enriched viruses can be linked to differences in the number of α1–2-linked mannoses on the *N*-glycans.

We showed that $HIV\text{-}1_{kif}$ was more efficiently captured and degraded by iDCs compared with $HIV\text{-}1_{wt}$. This can be explained by an enhanced affinity of $HIV\text{-}1_{kif}$ for mannose-specific CLRs, because CLRs, such as DC-SIGN, DCIR, and the mannose receptor, are known to target their ligands to early/late endosomes for Ag presentation (54–56). Therefore, changing the *N*-linked glycan composition of Ags into exclusively oligomannose *N*-glycans could aid protein subunit vaccination strategies. The oligomannose glycans can enhance Ag targeting to DCs and improve processing of Ags for induction Ag presentation to initiate T cell responses. However, under some circumstances, oligomannose glycans can also induce immune suppression (57–59), so the eventual outcome of the immune response is likely to be determined by several factors.

The hijacking of iDCs by HIV-1 in mucosal tissues and its transport to target T cells in secondary lymphoid organs provides a paradox, because binding of HIV-1 to CLRs, such as DC-SIGN, should lead to efficient internalization, Ag processing, and initiation of a potent immune response. The mechanisms by which HIV-1 manages to escape degradation in DCs and suppress DC function start to come unraveled (60). The data presented in this article illuminate how HIV-1 glycan composition plays a role in this process and determines how a DC treats an incoming virus (Fig. 10). There seem to be two checkpoints at which glycan composition plays a crucial role in deciding the fate of a virus. First, glycan composition determines whether a virus is captured (checkpoint A in Fig. 10). A virus with only complex glycans is unlikely to be captured efficiently by DCs, because it has a low or no affinity for C-type lectins, such as DC-SIGN. Hence, the virus requires a certain amount of oligomannose glycans. Following efficient virus capture by a DC, a second checkpoint determines the subsequent intracellular trafficking of a virus (checkpoint B at Fig. 10). HIV-1 can be treated as a classical pathogen that is degraded, and processed for Ag presentation, resulting in an antiviral immune response (pathway 1 in Fig. 10), or the virus can be preserved in a nonendocytic DC-compartment to be transferred to HIV-1–susceptible target cells (pathway 2 in Fig. 10). A high density of oligomannose glycans favors pathway 1 (Ag presentation), whereas a lower amount of oligomannose glycans favors pathway 2 (in

trans infection). Thus, oligomannose is required for lectin binding at checkpoint A, but too much oligomannose negatively affects the decision at checkpoint B.

In summary, HIV-1 maintains a glycan-governed balance between efficient virus capture and efficient virus preservation for in trans infection, while avoiding degradation and Ag presentation. These results may have implications for the early events in HIV-1 transmission and the induction of antiviral immune responses.

Acknowledgments

This work was supported by AIDS Fund (Amsterdam) Grants 2005021 (to B.B.) and 2008013 (to R.W.S.). R.W.S. is a recipient of Veni and Vidi fellowships from The Netherlands Organization for Scientific Research and a Mathilde Krim research fellowship from the American Foundation for AIDS Research.

We thank A.A.M. Thomas for critical reading of the manuscript, Ilja Bontjer and Stephan Heynen for technical assistance, and Bill Olson and Thomas Hope for reagents.

Abbreviations used in this article

CLR	C-type lectin receptor
DC	dendritic cell
DCIR	dendritic cell immunoreceptor
DC-SIGN	dendritic cell-specific ICAM-3–grabbing nonintegrin
EGFP	enhanced GFP
Env	envelope glycoprotein complex
ER	endoplasmic reticulum
GnTI	GlcNAc transferase I enzyme
iDC	immature dendritic cell
PEI	polyethylenimine
Raji–DC-SIGN cell	Raji cell expressing dendritic cell-specific ICAM-3–grabbing nonintegrin
TSM	tris saline magnesium buffer
wt	wild-type

References

1. Laurence J. Reservoirs of HIV infection or carriage: monocytic, dendritic, follicular dendritic, and B cells. Ann N Y Acad Sci. 1993; 693:52–64. [PubMed: 8267295]
2. Wilkinson J, Cunningham AL. Mucosal transmission of HIV-1: first stop dendritic cells. Curr Drug Targets. 2006; 7:1563–1569. [PubMed: 17168831]
3. Banchereau J, Steinman RM. Dendritic cells and the control of immunity. Nature. 1998; 392:245–252. [PubMed: 9521319]
4. Loré K, Sönnerborg A, Broström C, Goh LE, Perrin L, McDade H, Stellbrink HJ, Gazzard B, Weber R, Napolitano LA, et al. Accumulation of DC-SIGN+CD40+ dendritic cells with reduced CD80 and CD86 expression in lymphoid tissue during acute HIV-1 infection. AIDS. 2002; 16:683–692. [PubMed: 11964524]
5. Garcia E, Pion M, Pelchen-Matthews A, Collinson L, Arrighi JF, Blot G, Leuba F, Escola JM, Demaurex N, Marsh M, Piguet V. HIV-1 trafficking to the dendritic cell-T-cell infectious synapse

uses a pathway of tetraspanin sorting to the immunological synapse. Traffic. 2005; 6:488–501. [PubMed: 15882445]

6. Izquierdo-Useros N, Naranjo-Gómez M, Archer J, Hatch SC, Erkizia I, Blanco J, Borràs FE, Puertas MC, Connor JH, Fernández-Figueras MT, et al. Capture and transfer of HIV-1 particles by mature dendritic cells converges with the exosome-dissemination pathway. Blood. 2009; 113:2732–2741. [PubMed: 18945959]
7. McDonald D, Wu L, Bohks SM, KewalRamani VN, Unutmaz D, Hope TJ. Recruitment of HIV and its receptors to dendritic cell-T cell junctions. Science. 2003; 300:1295–1297. [PubMed: 12730499]
8. Turville SG, Santos JJ, Frank I, Cameron PU, Wilkinson J, Miranda-Saksena M, Dable J, Stössel H, Romani N, Piatak M Jr, et al. Immunodeficiency virus uptake, turnover, and 2-phase transfer in human dendritic cells. Blood. 2004; 103:2170–2179. [PubMed: 14630806]
9. Ganesh L, Leung K, Loré K, Levin R, Panet A, Schwartz O, Koup RA, Nabel GJ. Infection of specific dendritic cells by CCR5-tropic human immunodeficiency virus type 1 promotes cell-mediated transmission of virus resistant to broadly neutralizing antibodies. J Virol. 2004; 78:11980–11987. [PubMed: 15479838]
10. Hu J, Gardner MB, Miller CJ. Simian immunodeficiency virus rapidly penetrates the cervicovaginal mucosa after intravaginal inoculation and infects intraepithelial dendritic cells. J Virol. 2000; 74:6087–6095. [PubMed: 10846092]
11. Holl V, Peressin M, Decoville T, Schmidt S, Zolla-Pazner S, Aubertin AM, Moog C. Nonneutralizing antibodies are able to inhibit human immunodeficiency virus type 1 replication in macrophages and immature dendritic cells. J Virol. 2006; 80:6177–6181. [PubMed: 16731957]
12. Holl V, Peressin M, Schmidt S, Decoville T, Zolla-Pazner S, Aubertin AM, Moog C. Efficient inhibition of HIV-1 replication in human immature monocyte-derived dendritic cells by purified anti-HIV-1 IgG without induction of maturation. Blood. 2006; 107:4466–4474. [PubMed: 16469871]
13. van Montfort T, Thomas AA, Pollakis G, Paxton WA. Dendritic cells preferentially transfer CXCR4-using human immunodeficiency virus type 1 variants to CD4+ T lymphocytes in trans. J Virol. 2008; 82:7886–7896. [PubMed: 18524826]
14. Sallusto F, Cella M, Danieli C, Lanzavecchia A. Dendritic cells use macropinocytosis and the mannose receptor to concentrate macromolecules in the major histocompatibility complex class II compartment: downregulation by cytokines and bacterial products. J Exp Med. 1995; 182:389–400. [PubMed: 7629501]
15. Geijtenbeek TB, van Duijnhoven GC, van Vliet SJ, Krieger E, Vriend G, Figdor CG, van Kooyk Y. Identification of different binding sites in the dendritic cell-specific receptor DC-SIGN for intercellular adhesion molecule 3 and HIV-1. J Biol Chem. 2002; 277:11314–11320. [PubMed: 11799126]
16. Ariizumi K, Shen GL, Shikano S, Ritter R III, Zukas P, Edelbaum D, Morita A, Takashima A. Cloning of a second dendritic cell-associated C-type lectin (dectin-2) and its alternatively spliced isoforms. J Biol Chem. 2000; 275:11957–11963. [PubMed: 10766825]
17. Willment JA, Gordon S, Brown GD. Characterization of the human beta-glucan receptor and its alternatively spliced isoforms. J Biol Chem. 2001; 276:43818–43823. [PubMed: 11567029]
18. Bates EE, Fournier N, Garcia E, Valladeau J, Durand I, Pin JJ, Zurawski SM, Patel S, Abrams JS, Lebecque S, et al. APCs express DCIR, a novel C-type lectin surface receptor containing an immunoreceptor tyrosine-based inhibitory motif. J Immunol. 1999; 163:1973–1983. [PubMed: 10438934]
19. Ryan EJ, Marshall AJ, Magaletti D, Floyd H, Draves KE, Olson NE, Clark EA. Dendritic cell-associated lectin-1: a novel dendritic cell-associated, C-type lectin-like molecule enhances T cell secretion of IL-4. J Immunol. 2002; 169:5638–5648. [PubMed: 12421943]
20. Colonna M, Samaridis J, Angman L. Molecular characterization of two novel C-type lectin-like receptors, one of which is selectively expressed in human dendritic cells. Eur J Immunol. 2000; 30:697–704. [PubMed: 10671229]
21. Mahnke K, Guo M, Lee S, Sepulveda H, Swain SL, Nussenzweig M, Steinman RM. The dendritic cell receptor for endocytosis, DEC-205, can recycle and enhance antigen presentation via major

histocompatibility complex class II-positive lysosomal compartments. J Cell Biol. 2000; 151:673–684. [PubMed: 11062267]

22. Suzuki N, Yamamoto K, Toyoshima S, Osawa T, Irimura T. Molecular cloning and expression of cDNA encoding human macrophage C-type lectin. Its unique carbohydrate binding specificity for Tn antigen. J Immunol. 1996; 156:128–135. [PubMed: 8598452]
23. Turville SG, Cameron PU, Handley A, Lin G, Pöhlmann S, Doms RW, Cunningham AL. Diversity of receptors binding HIV on dendritic cell subsets. Nat Immunol. 2002; 3:975–983. [PubMed: 12352970]
24. Geijtenbeek TB, van Vliet SJ, Engering A, 't Hart BA, van Kooyk Y. Self- and nonself-recognition by C-type lectins on dendritic cells. Annu Rev Immunol. 2004; 22:33–54. [PubMed: 15032573]
25. Lambert AA, Gilbert C, Richard M, Beaulieu AD, Tremblay MJ. The C-type lectin surface receptor DCIR acts as a new attachment factor for HIV-1 in dendritic cells and contributes to trans- and cis-infection pathways. Blood. 2008; 112:1299–1307. [PubMed: 18541725]
26. van Montfort T, Nabatov AA, Geijtenbeek TB, Pollakis G, Paxton WA. Efficient capture of antibody neutralized HIV-1 by cells expressing DC-SIGN and transfer to CD4+ T lymphocytes. J Immunol. 2007; 178:3177–3185. [PubMed: 17312166]
27. Wang JH, Janas AM, Olson WJ, Wu L. Functionally distinct transmission of human immunodeficiency virus type 1 mediated by immature and mature dendritic cells. J Virol. 2007; 81:8933–8943. [PubMed: 17567699]
28. Feinberg H, Castelli R, Drickamer K, Seeberger PH, Weis WI. Multiple modes of binding enhance the affinity of DC-SIGN for high mannose N-linked glycans found on viral glycoproteins. J Biol Chem. 2007; 282:4202–4209. [PubMed: 17150970]
29. van Liempt E, Bank CM, Mehta P, Garciá-Vallejo JJ, Kawar ZS, Geyer R, Alvarez RA, Cummings RD, Kooyk Y, van Die I. Specificity of DC-SIGN for mannose- and fucose-containing glycans. FEBS Lett. 2006; 580:6123–6131. [PubMed: 17055489]
30. García-Vallejo JJ, van Liempt E, da Costa Martins P, Beckers C, van het Hof B, Gringhuis SI, Zwaginga JJ, van Dijk W, Geijtenbeek TB, van Kooyk Y, van Die I. DC-SIGN mediates adhesion and rolling of dendritic cells on primary human umbilical vein endothelial cells through LewisY antigen expressed on ICAM-2. Mol Immunol. 2008; 45:2359–2369. [PubMed: 18155766]
31. Reitter JN, Means RE, Desrosiers RC. A role for carbohydrates in immune evasion in AIDS. Nat Med. 1998; 4:679–684. [PubMed: 9623976]
32. Binley JM, Ban YE, Crooks ET, Eggink D, Osawa K, Schief WR, Sanders RW. Role of complex carbohydrates in human immunodeficiency virus type 1 infection and resistance to antibody neutralization. J Virol. 2010; 84:5637–5655. [PubMed: 20335257]
33. Sanders RW, van Anken E, Nabatov AA, Liscaljet IM, Bontjer I, Eggink D, Melchers M, Busser E, Dankers MM, Groot F, et al. The carbohydrate at asparagine 386 on HIV-1 gp120 is not essential for protein folding and function but is involved in immune evasion. Retrovirology. 2008; 5:10. [PubMed: 18237398]
34. Sagar M, Wu X, Lee S, Overbaugh J. Human immunodeficiency virus type 1 V1-V2 envelope loop sequences expand and add glycosylation sites over the course of infection, and these modifications affect antibody neutralization sensitivity. J Virol. 2006; 80:9586–9598. [PubMed: 16973562]
35. Walker BD, Kowalski M, Goh WC, Kozarsky K, Krieger M, Rosen C, Rohrschneider L, Haseltine WA, Sodroski J. Inhibition of human immunodeficiency virus syncytium formation and virus replication by castanospermine. Proc Natl Acad Sci USA. 1987; 84:8120–8124. [PubMed: 2825177]
36. Leonard CK, Spellman MW, Riddle L, Harris RJ, Thomas JN, Gregory TJ. Assignment of intrachain disulfide bonds and characterization of potential glycosylation sites of the type 1 recombinant human immunodeficiency virus envelope glycoprotein (gp120) expressed in Chinese hamster ovary cells. J Biol Chem. 1990; 265:10373–10382. [PubMed: 2355006]
37. Sanders RW, Venturi M, Schiffner L, Kalyanaraman R, Katinger H, Lloyd KO, Kwong PD, Moore JP. The mannose-dependent epitope for neutralizing antibody 2G12 on human immunodeficiency virus type 1 glycoprotein gp120. J Virol. 2002; 76:7293–7305. [PubMed: 12072528]
38. Eggink D, Melchers M, Wuhrer M, van Montfort T, Dey AK, Naaijkens BA, David KB, Le Douce V, Deelder AM, Kang K, et al. Lack of complex N-glycans on HIV-1 envelope glycoproteins

preserves protein conformation and entry function. Virology. 2010; 401:236–247. [PubMed: 20304457]

39. Sanders RW, Vesanen M, Schuelke N, Master A, Schiffner L, Kalyanaraman R, Paluch M, Berkhout B, Maddon PJ, Olson WC, et al. Stabilization of the soluble, cleaved, trimeric form of the envelope glycoprotein complex of human immunodeficiency virus type 1. J Virol. 2002; 76:8875–8889. [PubMed: 12163607]
40. Kirschner M, Monrose V, Paluch M, Techodamrongsin N, Rethwilm A, Moore JP. The production of cleaved, trimeric human immunodeficiency virus type 1 (HIV-1) envelope glycoprotein vaccine antigens and infectious pseudoviruses using linear polyethylenimine as a transfection reagent. Protein Expr Purif. 2006; 48:61–68. [PubMed: 16600625]
41. Cohen S, Tuen M, Hioe CE. Propagation of CD4+ T cells specific for HIV type 1 envelope gp120 from chronically HIV type 1-infected subjects. AIDS Res Hum Retroviruses. 2003; 19:793–806. [PubMed: 14585210]
42. Elbein AD, Tropea JE, Mitchell M, Kaushal GP. Kifunensine, a potent inhibitor of the glycoprotein processing mannosidase I. J Biol Chem. 1990; 265:15599–15605. [PubMed: 2144287]
43. Reeves PJ, Callewaert N, Contreras R, Khorana HG. Structure and function in rhodopsin: high-level expression of rhodopsin with restricted and homogeneous N-glycosylation by a tetracycline-inducible N-acetylglucosam-inyltransferase I-negative HEK293S stable mammalian cell line. Proc Natl Acad Sci USA. 2002; 99:13419–13424. [PubMed: 12370423]
44. Geijtenbeek TB, Kwon DS, Torensma R, van Vliet SJ, van Duijnhoven GC, Middel J, Cornelissen IL, Nottet HS, KewalRamani VN, Littman DR, et al. DC-SIGN, a dendritic cell-specific HIV-1-binding protein that enhances trans-infection of T cells. Cell. 2000; 100:587–597. [PubMed: 10721995]
45. Scanlan CN, Pantophlet R, Wormald MR, Ollmann Saphire E, Stanfield R, Wilson IA, Katinger H, Dwek RA, Rudd PM, Burton DR. The broadly neutralizing anti-human immunodeficiency virus type 1 antibody 2G12 recognizes a cluster of alpha1→2 mannose residues on the outer face of gp120. J Virol. 2002; 76:7306–7321. [PubMed: 12072529]
46. Sugaya M, Loré K, Koup RA, Douek DC, Blauvelt A. HIV-infected Langerhans cells preferentially transmit virus to proliferating autologous CD4+ memory T cells located within Langerhans cell-T cell clusters. J Immunol. 2004; 172:2219–2224. [PubMed: 14764689]
47. Garcia E, Nikolic DS, Piguet V. HIV-1 replication in dendritic cells occurs through a tetraspanin-containing compartment enriched in AP-3. Traffic. 2008; 9:200–214. [PubMed: 18034776]
48. Montefiori DC, Robinson WE Jr, Mitchell WM. Role of protein N-glycosylation in pathogenesis of human immunodeficiency virus type 1. Proc Natl Acad Sci USA. 1988; 85:9248–9252. [PubMed: 3264072]
49. Pal R, Hoke GM, Sarngadharan MG. Role of oligosaccharides in the processing and maturation of envelope glycoproteins of human immunodeficiency virus type 1. Proc Natl Acad Sci USA. 1989; 86:3384–3388. [PubMed: 2541446]
50. de Witte L, Bobardt M, Chatterji U, Degeest G, David G, Geijtenbeek TB, Gallay P. Syndecan-3 is a dendritic cell-specific attachment receptor for HIV-1. Proc Natl Acad Sci USA. 2007; 104:19464–19469. [PubMed: 18040049]
51. Bobardt MD, Saphire AC, Hung HC, Yu X, Van der Schueren B, Zhang Z, David G, Gallay PA. Syndecan captures, protects, and transmits HIV to T lymphocytes. Immunity. 2003; 18:27–39. [PubMed: 12530973]
52. Magérus-Chatinet A, Yu H, Garcia S, Ducloux E, Terris B, Bomsel M. Galactosyl ceramide expressed on dendritic cells can mediate HIV-1 transfer from monocyte derived dendritic cells to autologous T cells. Virology. 2007; 362:67–74. [PubMed: 17234232]
53. Guo Y, Feinberg H, Conroy E, Mitchell DA, Alvarez R, Blixt O, Taylor ME, Weis WI, Drickamer K. Structural basis for distinct ligand-binding and targeting properties of the receptors DC-SIGN and DC-SIGNR. Nat Struct Mol Biol. 2004; 11:591–598. [PubMed: 15195147]
54. Engering AJ, Cella M, Fluitsma DM, Hoefsmit EC, Lanzavecchia A, Pieters J. Mannose receptor mediated antigen uptake and presentation in human dendritic cells. Adv Exp Med Biol. 1997; 417:183–187. [PubMed: 9286359]

55. Engering A, Geijtenbeek TB, van Vliet SJ, Wijers M, van Liempt E, Demaurex N, Lanzavecchia A, Fransen J, Figdor CG, Piguet V, van Kooyk Y. The dendritic cell-specific adhesion receptor DC-SIGN internalizes antigen for presentation to T cells. J Immunol. 2002; 168:2118–2126. [PubMed: 11859097]

56. Meyer-Wentrup F, Benitez-Ribas D, Tacken PJ, Punt CJ, Figdor CG, de Vries IJ, Adema GJ. Targeting DCIR on human plasmacytoid dendritic cells results in antigen presentation and inhibits IFN-alpha production. Blood. 2008; 111:4245–4253. [PubMed: 18258799]

57. Banerjee K, Andjelic S, Klasse PJ, Kang Y, Sanders RW, Michael E, Durso RJ, Ketas TJ, Olson WC, Moore JP. Enzymatic removal of mannose moieties can increase the immune response to HIV-1 gp120 in vivo. Virology. 2009; 389:108–121. [PubMed: 19410272]

58. Martinelli E, Cicala C, Van Ryk D, Goode DJ, Macleod K, Arthos J, Fauci AS. HIV-1 gp120 inhibits TLR9-mediated activation and IFN-alpha secretion in plasmacytoid dendritic cells. Proc Natl Acad Sci USA. 2007; 104:3396–3401. [PubMed: 17360657]

59. Shan M, Klasse PJ, Banerjee K, Dey AK, Iyer SP, Dionisio R, Charles D, Campbell-Gardener L, Olson WC, Sanders RW, Moore JP. HIV-1 gp120 mannoses induce immunosuppressive responses from dendritic cells. PLoS Pathog. 2007; 3:e169. [PubMed: 17983270]

60. Lorenzo ME, Ploegh HL, Tirabassi RS. Viral immune evasion strategies and the underlying cell biology. Semin Immunol. 2001; 13:1–9. [PubMed: 11289794]

61. Cutalo JM, Deterding LJ, Tomer KB. Characterization of glycopeptides from HIV-I(SF2) gp120 by liquid chromatography mass spectrometry. J Am Soc Mass Spectrom. 2004; 15:1545–1555. [PubMed: 15519221]

62. Zhu X, Borchers C, Bienstock RJ, Tomer KB. Mass spectrometric characterization of the glycosylation pattern of HIV-gp120 expressed in CHO cells. Biochemistry. 2000; 39:11194–11204. [PubMed: 10985765]

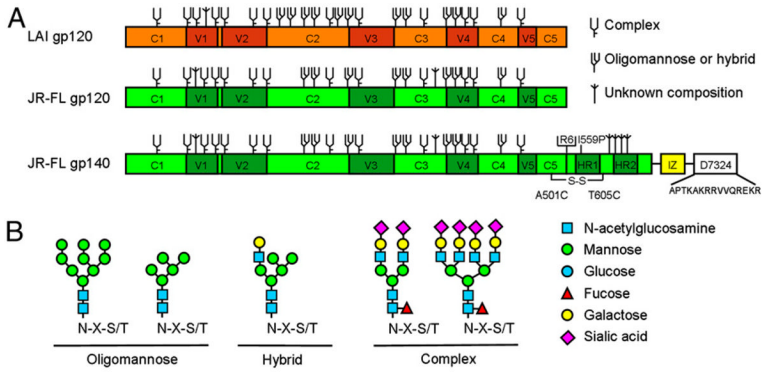

FIGURE 1.

Study design. *A*, The gp120 and gp140 proteins used in this study. Constructs are based on the sequences from LAI and JR-FL, indicated in orange and green, respectively. Trimeric JR-FL SOSIP.R6-IZ-D7324 gp140 contains several modifications that were described elsewhere (38). A variant, JR-FL SOSIP.R6-IZ-His gp140, does not contain the D7324 epitope tag, but a His tag. The *N*-linked glycan sites on gp120 produced in wt mammalian cells are designated as oligomannose or complex, based on experimental determinations using IIIB gp120 (36). It is assumed that the glycans present at analogous sites are processed similarly on LAI and JR-FL gp120, but we noted that the *N*-glycan type (oligomannose versus complex) present at some sites depends on the study and isolate used (36, 61, 62). Furthermore, some sites can be unoccupied in a subset of molecules or be occupied by both complex and oligomannose sugars (61, 62). Sites that are present on LAI or JR-FL gp120, but not on IIIB gp120, are designated as being of unknown glycan composition. *B*, The composition of a representative subset of oligomannose, hybrid, or complex *N*-linked glycans.

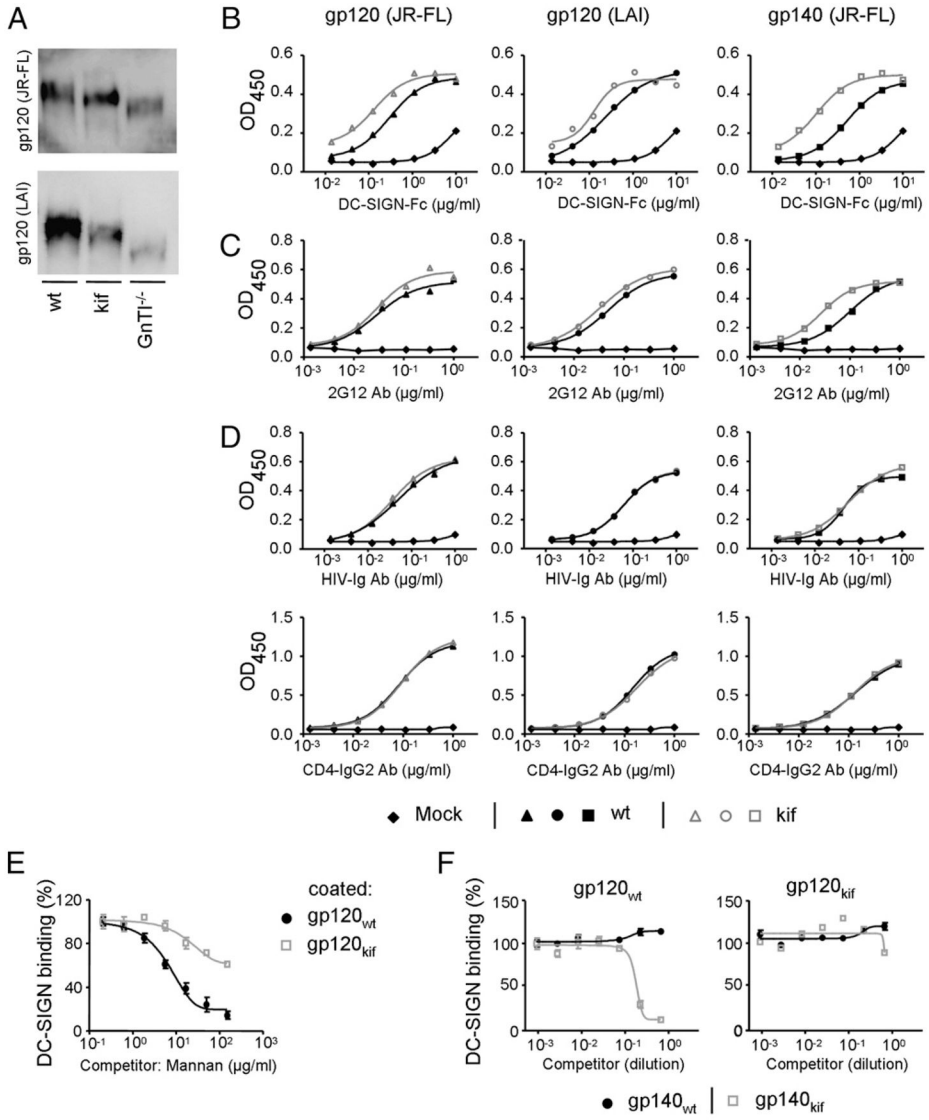

FIGURE 2.

Enrichment of oligomannose *N*-glycans on Env enhances DC-SIGN binding. *A*, SDS-PAGE analysis of gp120 expressed on 293T cells in the absence (wt) or presence of kifunensine (kif) or on 293S GnTI$^{-/-}$ cells transfected with plasmid DNA encoding JR-FL or LAI gp120. ELISA analysis of the binding of DC-SIGN (*B*), 2G12 (*C*), or HIV-Ig and CD4-IgG2 (*D*) to JR-FL gp120 (*left panels*), LAI gp120 (*middle panels*), or JR-FL gp140 (SOSIP. R6-IZ-D7324; *right panels*). Env produced in the absence (black lines) or presence (gray lines) of kifunensine is depicted. Mock medium (◆) served as negative control. *E*, Competition of mannan for DC-SIGN binding to gp120 expressed in 293T cells in the absence (●) or presence (□) of kifunensine. DC-SIGN (1.0 μg/ml) was preincubated with serially diluted mannan prior to addition to the JR-FL gp120, which was precoated onto the ELISA plate. *F*, Competition of trimeric JR-FL gp140 (JR-FL SOSIP.R6-IZ-His) expressed in 293T cells in the absence (●) or presence (□) of kifunensine for DC binding to immobilized gp120 expressed in 293T cells in the absence (*left panel*) or presence (*right panel*) of kifunensine. DC-SIGN (1.0 μg/ml) was preincubated with serially diluted gp140-containing supernatant prior to addition to the gp120, which was precoated onto the ELISA plate. The JR-FL gp140

trimer used for the experiments in *F* (SOSIP.R6-IZ-His) did not contain the D7324 epitope tag to prevent binding to the ELISA capture Ab D7324.

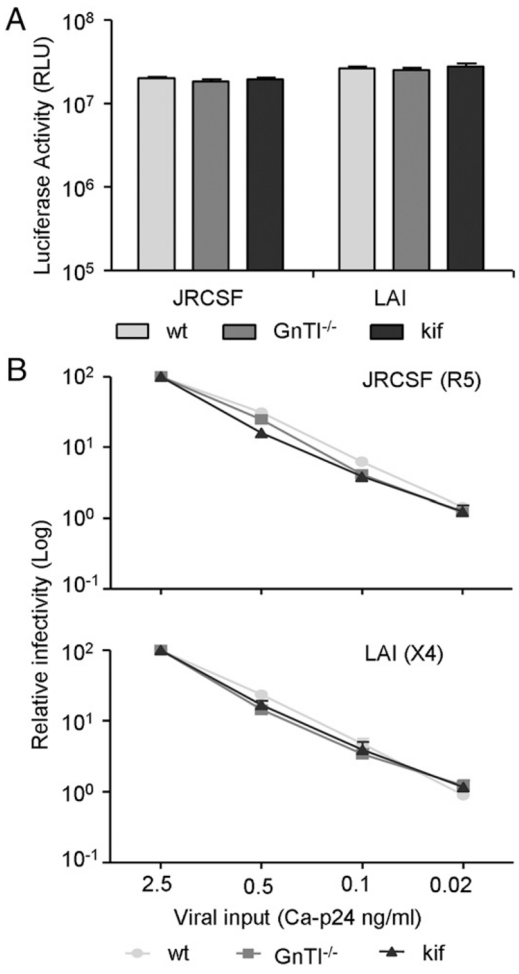

FIGURE 3.

N-glycan manipulation does not affect HIV-1 infectivity. *A*, JR-CSF and LAI viruses were produced in 293T cells in the absence or presence of kifunensine or in GnTI$^{-/-}$ cells. TZM-bl cells were inoculated with viral supernatant normalized for CA-p24, and viral infectivity was quantified by measuring the luciferase activity. *B*, Infection of TZM-bl cells by 5-fold serially diluted virus normalized for CA-p24 protein was measured and normalized to the highest input concentration. Data represent the mean of quadruplicate wells.

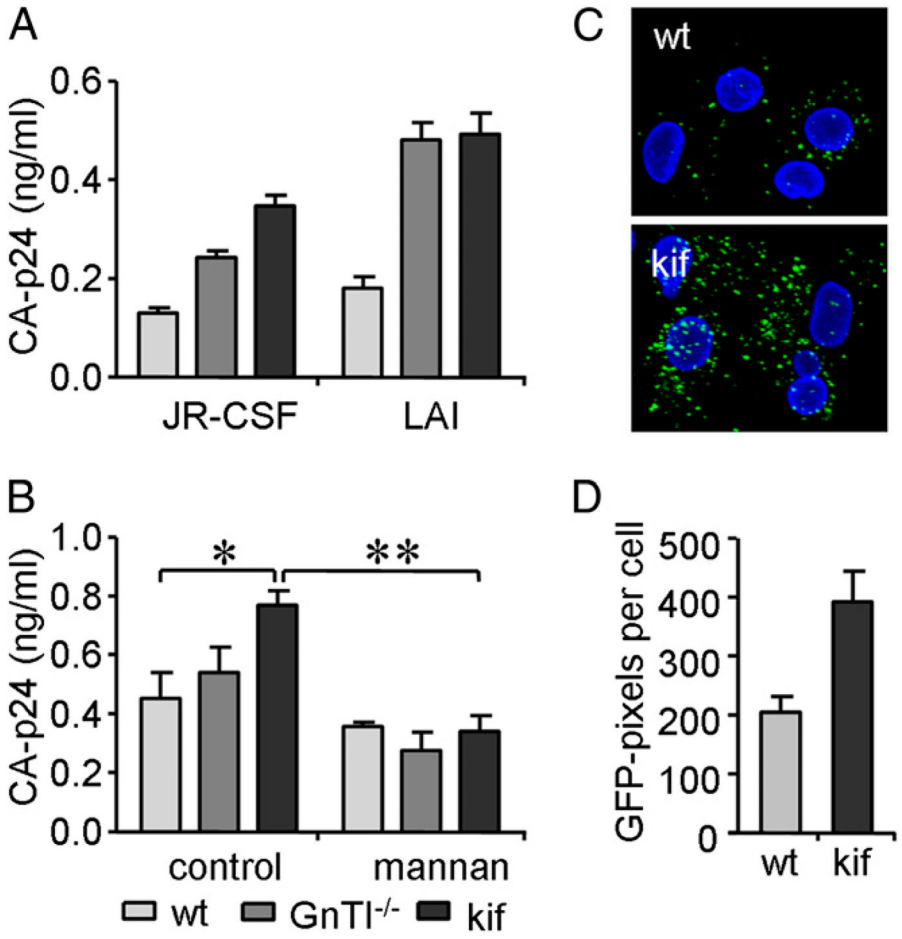

FIGURE 4.

Enrichment of oligomannose *N*-glycans enhances virus capture by Raji–DC-SIGN cells and immature DCs. *A*, Raji–DC-SIGN cells were incubated for 2 h with JR-CSF or LAI produced in 293T cells either in the presence (black) or absence (light gray) of kifunensine or in GnTI$^{-/-}$ cells (dark gray). Cells were washed, and captured viral CA-p24 protein was measured by ELISA. *B*, iDCs were incubated for 2 h with wt, GnTI$^{-/-}$, or kifunensine (kif) JR-CSF virus. Viral capture in the presence or absence of mannan was determined by measuring bound CA-p24 by ELISA. Data represent the mean ± SD of triplicate wells. *C*, GFP-fluorescent JR-CSF virus produced in the absence (wt) or presence of kifunensine (kif) was mixed for 2 h with iDCs. Images of GFP JR-CSF (green) loaded iDCs were visualized by confocal microscopy (original magnification ×126). Nuclei were stained by Hoechst (blue). *D*, The mean (± SEM) GFP-signal intensity was determined by measuring the number of GFP^{+} pixels/cell for ~200 cells. Gray bars represent the signal of virus produced without kifunensine, and black bars represent the virus produced with kifunensine. *$p < 0.05$, **$p < 0.01$.

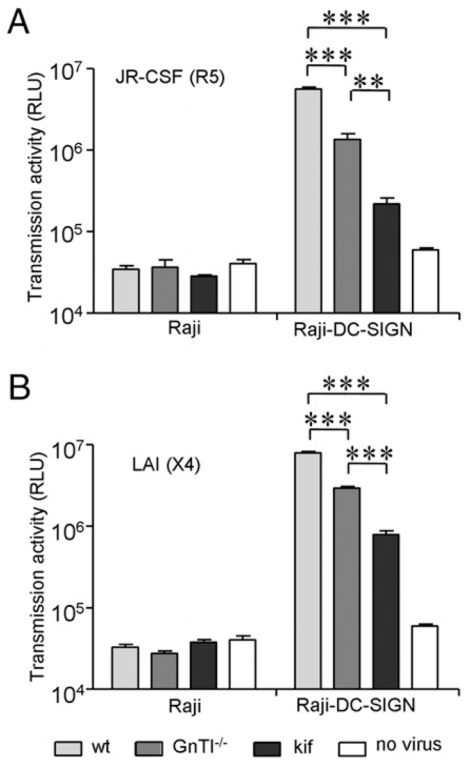

FIGURE 5.

Enrichment of oligomannose glycans reduces viral transmission from Raji–DC-SIGN to target cells. Raji and Raji–DC-SIGN cells were loaded with wt (light gray), GnTI$^{-/-}$ (dark gray) and kifunensine (black) virus from the JR-FL (*A*) and LAI strain (*B*). Unbound virus was washed, and viral transmission to HIV-1–susceptible TZM-bl cells was determined by measuring the luciferase activity. Background luciferase activity was determined by coculturing Raji or Raji–DC-SIGN cells without virus with TZM-bl cells (white). Data represent the mean (± SD) luciferase activity from four independent wells. ***$p < 0.001$.

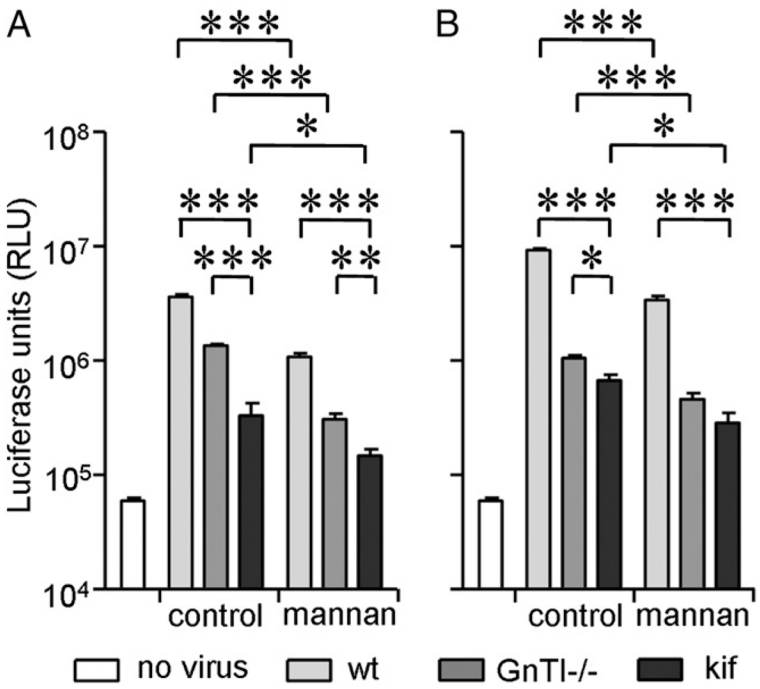

FIGURE 6.

Enrichment of oligomannose glycans reduces viral transmission from iDCs to target cells. iDCs were loaded for 2 h with 293T wt-, GnTI$^{-/-}$-, or kifunensine-produced virus in the presence or absence of mannan. *A*, Viral transfer of the CCR5-tropic JR-CSF strain from iDCs to TZM-bl cells. Data (mean ± SD) are representative of three independent cocultures. Background luciferase activity was determined by coculturing iDCs inoculated with medium with TZM-bl cells. *B*, Viral transfer of CXCR4-using LAI by iDCs. *$p < 0.05$, **$p < 0.01$, ***$p < 0.001$.

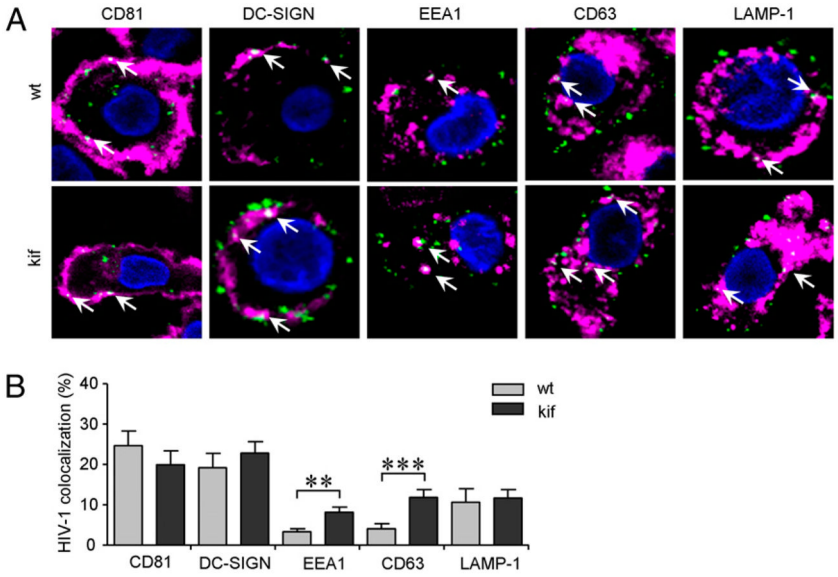

FIGURE 7.

Oligomannose-enriched virus colocalizes more strongly with internal endocytic markers compared with wt virus. iDCs were loaded with fluorescent JR-CSF–GFP–labeled virus produced in 293T cells in the absence (wt) or presence with kifunensine (kif) for 2 h. Nuclei (blue) and different marker proteins specific for cellular compartments of iDCs were stained (pink); colocalization (white) with fluorescent HIV-1 (green) is indicated by arrows. *A*, The middle section of a representative single iDC in a confocal plane is shown (original magnification ×126). *B*, Colocalization of HIV-1 with the protein markers for iDCs was quantified from raw data using a semiautomatic program. Signal thresholding was performed according to Isodata algorithm, and colocalization was determined as the number of positive overlapping pixels from different channels of each Z-stack for single cells. A total ~50–60 cells was analyzed for each marker. Data are shown as the mean (± SEM) percentage of virus in each compartment of two independent experiments. Note that the contrast of the images in *A* was enhanced to improve visualization, but the calculations in *B* were performed on raw, unsaturated data.

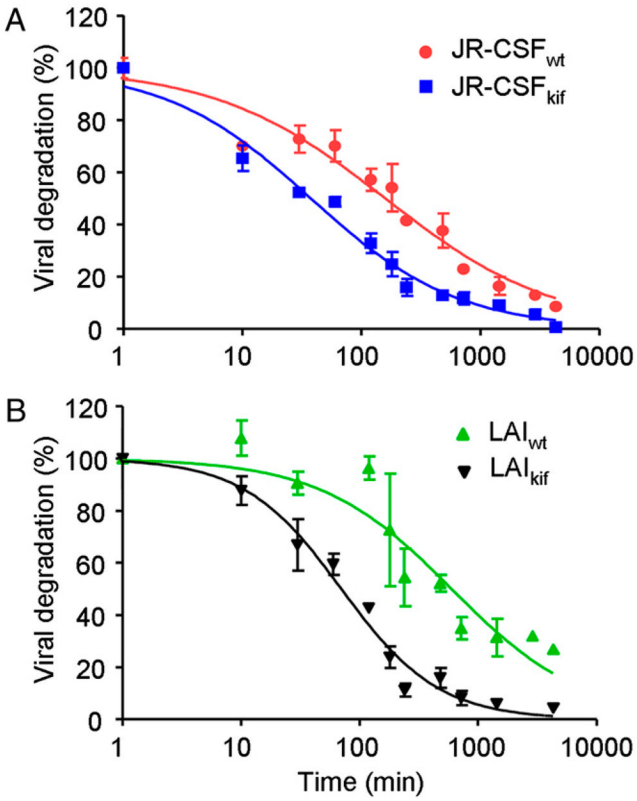

50% degradation time in min (t1/2)

	wt	kif
JR-CSF	159	38
LAI	599	70

FIGURE 8.

iDCs degrade oligomannose-enriched virus faster than wt virus. iDCs were incubated for 2 h with JR-CSF (*A*) or LAI (*B*) produced in 293T cells in the presence or absence of kifunensine. Unbound virus was washed, and viral degradation was determined by measuring the amount of CA-p24 at different incubation time periods. The percentage of HIV-1 degradation in time (min) was normalized. The elapsed time (min) when 50% of the captured virus was degraded by iDCs ($t_{1/2}$) was calculated using Prism 5.0 software. The experiment was performed twice with similar outcomes. The p values were < 0.0001 (using two-way ANOVA) for both JR-CSF (*A*) and LAI (*B*) viruses.

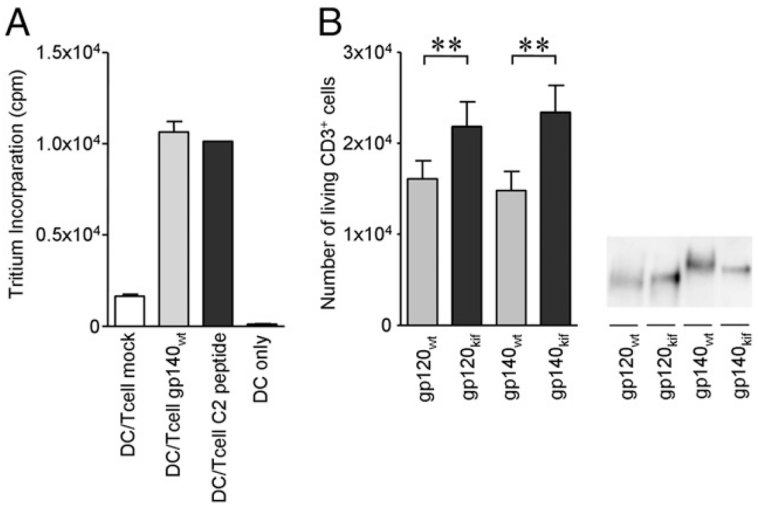

FIGURE 9.

Oligomannose enrichment of the envelope glycoprotein enhances DC-mediated proliferation of cognate T cells. *A*, iDCs mixed with PS02 T cells were cultured in the presence of mock medium or Env-or C2 peptide-containing medium. PS02 T cell proliferation was measured by detecting [^{3}H]thymidine tritium incorporation after 48 h. *B*, iDCs were loaded with monomeric or trimeric Env produced in the presence or absence of kifunensine. Unbound Env was washed away, and PS02 T cells were added to the iDC cultures. The number of living PS02 T cells positive for CD3 in 50 μl were counted using FACS flow cytometry. CD3 was used to distinguish the T cells from DCs. *Right panel*, SDS-PAGE analysis of the Env-containing supernatants used for PS02 stimulation. $^{**}p < 0.01$.

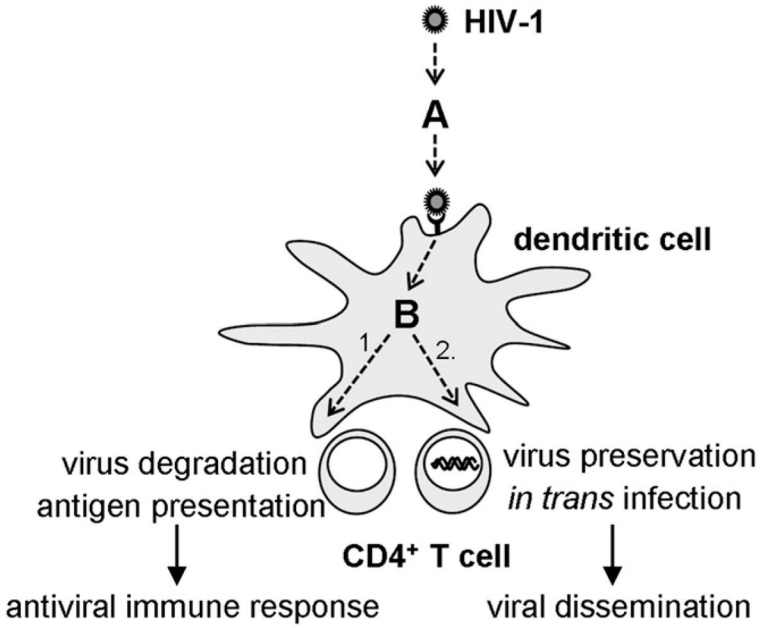

FIGURE 10.
The role of *N*-linked glycans in virus capture, transmission, degradation, and Ag presentation by iDCs.